Eco. Env. & Cons. 27 (2) : 2021; pp. (539-547)
Copyright@ EM International
ISSN 0971–765X

Production of calcium oxide from waste oyster shells for a value-added application of antibacteria

Suree Tongwanichniyom[1]*, Thanit Pattamapitoon[2], Napimporn Sangvichien[1] and Somkiat Phornphisutthimas[3]*

[1]Faculty of Science at Sriracha, Kasetsart University, Chonburi 20230, Thailand
[2]Faculty of Environment, Environmental Science, Kasetsart University, Bangkok 10900, Thailand
[3]Department of Biology, and Research Unit on Science, Technology and Environment for Learning, Faculty of Science, Srinakharinwirot University, Bangkok 10110, Thailand

(Received 17 September, 2020; Accepted 2 October, 2020)

ABSTRACT

The production of calcium oxide was investigated from waste oyster shells as a value-added application in inhibiting bacteria. Oyster shell powder was prepared in 4 forms: natural oyster shell powder (NOSP) and calcined in a programmable furnace for 2 hours at 700°C (OSP_{700}), 800°C (OSP_{800}) and 900°C (OSP_{900}). All forms were analyzed for physical properties using thermogravimetric analysis, X-ray diffraction and Fourier-transformed infrared spectrometry. The results indicated that the calcium carbonate of NOSP, OSP_{700} and OSP_{800} had a rhombohedral structure of calcite. On the other hand, the calcium carbonate structure of OSP_{900} changed to calcium oxide (CaO) and calcium hydroxide ($Ca(OH)_2$). The findings were consistent with the Fourier-transformed infrared spectrometry results as they showed the peak of C–O stretching, indicating a calcite structure, whereas the characteristics of the Ca=O group and O–H stretching of the functional group indicated the structures of CaO and $Ca(OH)_2$. OSP_{900} showed qualitative antibacterial activity by its inhibition zone on NA medium. Quantitatively, OSP_{900} had the highest antibacterial activity against *Escherichia coli* and *Staphylococcus aureus* at concentrations of 0.5% and 1.0% w/v, respectively, with significant differences for an exposure time of 30 minutes. In addition, OSP_{900} gave the best inhibition of *E. coli* in contaminated vegetables at a concentration of 0.5% w/v. The results of this study revealed the usefulness of OSP_{900} for further antibacterial applications in contaminated vegetables.

Key words : *Calcium oxide, Waste oyster shell, Antibacteria, Calcium carbonate, Saccostrea cucullata*

Introduction

Thailand has a highly developed fisheries industry, including cultivation, transportation, and processing of seafood. In particular, the cultivation of *Saccostrea cucullata* along the coast of eastern Thailand is well developed. A 2017 survey of the oyster culture reported that Chonburi province alone produced 5,452,000 kg, increasing 98% from 2015. *Saccostrea cucullata* is a nutritious seafood, so it is very popular among consumers (Fisheries Statistics of Thailand, 2017), resulting in increasingly large quantities of waste as shells along the coastline that are left to decompose naturally but this is considered unhygienic disposal. Recycling of the waste oyster shells is possible since oyster shell contains about 96% calcium carbonate ($CaCO_3$) (Yoon *et al.*, 2003). When the oyster shell is heated at 700°C or above, the calcium carbonate structure changes to calcium oxide (CaO) (Alidoust *et al.*, 2015). When dissolved or exposed to moisture further changes to calcium hydroxide ($Ca(OH)_2$) (Miller *et al.*, 2012), it is a bacterial inhibitor (Oikawa *et al.*, 2000).

Since vegetables are an agricultural product, they

***Corresponding author's email:** suree.to@ku.th; somkiatp@g.swu.ac.th

are often contaminated with bacteria during planting, harvesting, and transportation operations. In addition, Thailand has hot and humid weather that is suitable for the growth and easy spread of bacteria in the environment. Bacterial contamination in vegetables is often the major cause of gastrointestinal disease in public health (Nataro *et al.,* 2011) such as from *Staphylococcus aureus* (*S. aureus*), a Gram-positive bacterium causing acute food poisoning, diarrhea and dermatitis (Tapaneeyakul and Kongsuk, 2015). In addition, *Escherichia coli* (*E. coli*), a Gram-negative bacterium causing food poisoning, diarrhea and gastrointestinal disease. Based on such data, researchers have been interested in turning large quantities of waste oyster shells into more valuable substances that can replace synthetic chemicals and antiseptics. At present, only a few reports on the use of waste oyster shells are available, especially regarding public health, hygiene and the removal of bacterial contamination in vegetables.

The current study aimed to add value to waste oyster shells of *Saccostrea cucullata*, by producing calcium oxide for application in inhibiting the Gram-positive bacterium *S. aureus* ATCC 25922 and the Gram-negative bacterium *E. coli* ATCC 25923. In addition, CaO from *Saccostrea cucullata* was applied as a natural vegetable leaching material to reduce contamination of *E. coli* in fresh vegetables before consumption.

Materials and Methods

Preparation of oyster shell powder

The waste oyster shells used in this study were collected at seaside Ang Sila, Chonburi province, Thailand. The shells were cleaned by brushes after discarding the fresh remnant attached to them first. Then, they were washed with deionized water, air-dried at 60°C overnight, ground by a stone mortar and passed through 250 micrometers nylon sieves to provide natural oyster shell powder (NOSP) (Tsou *et al*., 2018).

Study on properties of oyster shell powder

The prepared oyster shell powder was calcined at 700°C (OSP_{700}), 800°C (OSP_{800}) and 900°C (OSP_{900}) in a high temperature furnace (Chawatchot L9/12P, Thailand) for 2 hours. Then, samples of NOSP, OSP_{700}, OSP_{800} and OSP_{900} were analyzed for physical characteristic changes and acidity (pH). The change in percent weight loss was calculated using equation (1) (Dangkanid, 1995):

$$\text{Weight loss (\%)} = \frac{\text{(initial weight – final weight)}}{\text{initial weight}} \times 100 \quad (1)$$

Then the powder samples were analyzed for thermal characteristics using a thermogravimetric analysis (TGA; Pyris Diamond, Perkin Elmer, USA), for crystalline structure using an X-ray diffraction (XRD; D8 Advance, Bruker AXS, Germany), and for chemical functional groups using Fourier-transformed infrared spectrometry (FTIR; FTIR-4100, JASCO, Spain).

Preparation of bacteria

The bacteria used in the laboratory experiment were prepared using *Escherichia coli* ATCC 25922 and *Staphylococcus aureus* ATCC 25923 from the Department of Medical Science, Ministry of Public Health, Thailand (DMSC). Each species of the bacteria was suspended in nutrient broth (NB) at 37°C for 24 hours. Bacterial samples were then transferred into 0.85% normal saline solution, and adjusted a density to about $1x10^8$ CFU/mL with McFarland standard No. 0.5 (Roy *et al.,* 2013).

Testing antibacterial activity

Qualitative antibacterial activity was tested against *E. coli* and *S. aureus* using the halo test with 0.1 mL of a cell suspension described above was spread thoroughly on nutrient agar (NA). The NOSP, OSP_{700}, OSP_{800} and OSP_{900} solutions were prepared by dissolving in aseptic distilled water to concentrations of 1, 2, 3, 4 and 5% w/v. Each paper disc was soaked in one of the different concentrations and then exposed to bacteria cultured with NA, followed by incubation at 37°C for 24 hours. Each test was replicated 4 times. The inhibition zone around the paper disc was measured and calculated according to equation (2) (Kositchaiyong *et al.,* 2010):

$$R_a = \frac{D_c - D_s}{2} \quad \text{In this equation,} \quad .. (2)$$

In this equation R_a is the inhibition zone (mm), D_c is the transparent diameter (mm) and D_s is the diameter of the paper disc (mm).

Quantitative antibacterial activity was tested against *E. coli* and *S. aureus* using the plate count technique on plate count agar (PCA) adapted from

the ASTM E2149-01 standard by dissolving OSP_{900} in NB at concentrations of 0, 0.025, 0.05, 0.1, 0.5, 0.75 and 1.0% w/v. Then, samples (1 mL) of the prepared *E. coli*, and *S. aureus* were added and shaken at 170 rpm and 37°C for 5 and 30 minutes. Subsequently, ten-fold serial dilutions (0.1 mL) were pipetted and spread thoroughly on the PCA surface, followed by incubation at 37°C for 24 hours. The procedure was repeated 4 times. The numbers of colonies were counted and represented in colony forming units per milliliter (CFU/mL) according to equation (3) by (Chammanee *et al.*, 2009) and used to calculate the percentage ability to inhibit bacteria according to equation (4):

$$CFU/mL = \frac{A}{10^n \times B} \quad .. (3)$$

In this equation A is the average of bacterial group, n is the number of dilution times and B is the volume of bacterial solution (0.1 mL).

$$\text{Antibacterial activity (\%)} = \frac{C - D}{C} \times 100 \quad .. (4)$$

In this equation, C is the number of bacteria surviving after testing (no oyster shell powder added), and D is the number of bacteria surviving after testing (oyster shell powder added).

Statistical analysis

Statistical analysis was performed using one-way analysis of variance (ANOVA) to compare the antibacterial activity against *E.coli* and *S. aureus* for OSP_{900} at different concentrations based on the SPSS 17.0 software package to differentiate the antibacterial activity. The significance level was at $p = 0.05$ level.

Test for antibacterial activity in vegetables

Antibacterial activity was tested against *E. coli* in vegetables by counting the colonies of infection on Eosin-methylene blue agar (EMB) as adapted from the American Public Health Association Compendium of Methods for the Microbiological Examination of Foods (2015). First, 1 g of bean sprouts and 1 g of lettuce were soaked in OSP_{900} solution at concentrations of 0, 0.25, 0.5 and 1% w/v for 5 minutes, then soaked in 0.85% normal saline solution. Ten-fold serial dilutions (0.1 mL) were pipetted and spreading on EMB agar. Each spread plate was incubated at 37°C for 24 hours. The procedure was repeated 4 times. Then, the numbers of colonies were counted and the colony forming units per milliliter (CFU/mL) were determined according to equation (3) (Chammanee *et al.*, 2009) and the percentage of antibacterial activity was calculated using equation (4).

Results and Discussion

Physical characteristics of oyster shell powder

The physical characteristics of oyster shell powder are shown in Figure 1 and Table 1. The outer shell was a dark grayish color with a hard, thick, and rough surface (Figure 1A) that turned to dark gray when crushed and sifted (Figure 1B). After calcination at 700°C (OSP_{700}) and 800°C (OSP_{800}), the weight of the shell powder reduced by 3.93% and 21.38%, respectively, the color changed to light gray and the sample became brittle (Figure 1C, 1D). Following calcination at 900°C, the weight lost by 76.10%, and the color changed to white and the sample became brittle (Figure 1E). The percentages of weight loss after the shell powder had been calcined were consistence with Boonyuen *et al.* (2015). The oyster shell powder calcined at low temperatures had only a slight reduction in weight unlike the calcinations at high temperature. The changes in color and weight of the shell powder were caused by high tempera-

(A) (B) (C) (D) (E)

Fig. 1. Physical characteristics of oyster shell (A), natural oyster shell powder (NOSP) (B), oyster shell powder calcined at 700°C (OSP_{700}) (C), oyster shell powder calcined at 800°C (OSP_{800}) (D), and oyster shell powder calcined at 900°C (OSP_{900}) (E)

ture calcination that induced oxidation reactions while releasing heat. At the same time, the calcium carbonate decayed to calcium oxide and carbon dioxide as described in the equation (5):

Table 1. Physical characteristics and weight loss of NOSP, OSP_{700}, OSP_{800} and OSP_{900}

Sample	Physical characteristic		
	Color	Softness	Weight loss (%)
NOSP	Dark gray	Hardness	-
OSP_{700}	Light gray	Brittle	3.93
OSP_{800}	Light gray	Brittle	21.38
OSP_{900}	White	Brittle	76.10

Note: NOSP = natural oyster shell powder, OSP_{700} = oyster shell powder calcined at 700°C, OSP_{800} = oyster shell powder calcined at 800°C, and OSP_{900} = oyster shell powder calcined at 900°C.

$$CaCO_3\ (s) \xrightarrow{\Delta} CaO\ (s) + CO_2\ (g) \quad .. (5)$$

Table 2 shows that oyster shell powder had an alkaline condition (pH > 7) both before and after calcination. The alkalinity increased with increases in the percentage of concentration and calcination temperature of NOSP, OSP_{700}, OSP_{800}, and OSP_{900}. For OSP_{900} at a concentration of 1.0%, the maximum alkalinity was 12.56 and was consistent with the results of Yen and Li (2015). When oyster shell powder was calcined at 900°C, the proportion of minerals in the oyster shell powder changed with calcium carbonate (a mild alkali) changing to calcium oxide and calcium hydroxide that has higher alkalinity.

NOSP was analyzed for thermal properties using TGA to study the behavior of the oyster shell after calcination from 40 to 1,000°C with increments of 10°C per minute. The results of the analysis (Figure 2) showed that NOSP went through 2 temperature ranges. For the temperature range 40.0-635.6°C, the weight of the oyster shell was 4% lower, as organic matter in the oyster shell changed to carbon and then ash at higher temperature. On the other hand, for the temperature range 635.6-704.8°C, the weight of the oyster shell decreased by 41.57% by weight as the structure of the shell changed from calcium carbonate to calcium oxide.

Table 2. Acidity of NOSP, OSP_{700}, OSP_{800} and OSP_{900} at different concentrations

Sample concentration (% w/v)	pH level			
	NOSP	OSP_{700}	OSP_{800}	OSP_{900}
0.025	9.36	10.12	11.72	12.07
0.05	9.44	10.77	11.97	12.12
0.10	9.52	11.11	12.17	12.37
0.50	9.63	12.01	12.45	12.51
0.75	9.68	12.16	12.50	12.52
1.0	9.69	12.24	12.51	12.56

Note: NOSP = natural oyster shell powder, OSP_{700} = oyster shell powder calcined at 700°C, OSP_{800} = oyster shell powder calcined at 800°C and OSP_{900} = oyster shell powder calcined at 900°C.

The changes in the crystalline structure of the crushed shell observed using XRD (Figure 3), showed that NOSP, OSP_{700} and OSP_{800} had primarily a calcium carbonate structure characterized by a rhombohedral, R-3C (167) pattern. X-ray diffraction patterns were detected at an angle of 2θ equal to 23.0°, 29.4°, 31.5°, 36.0°, 39.4°, 43.2°, 47.4° and 48.5°which were consistent with the JCPDS database no.05-0586. The results were consistent with the small changes in the percentage weights shown in Table 1.

Calcination at lower temperatures only removed the organic compounds; therefore, the crystalline structure did not change. On the other hand, there were structural changes for OSP_{900} (from calcium carbonate to calcium oxide), with the X-ray diffraction patterns detected at an angle of 2θ equal to 32.2°, 37.5°, 54.0°, 64.2° and 67.5°, which were consistent with the JCPDS database no. 78-0649. With the subsequent change to calcium hydroxide, the X-ray diffraction patterns at 2θ were 28.6°, 34.1°, 47.1° and 50.8°, which were consistent with the JCPDS database no. 76-0570. These findings differed from Boonyuen *et al.* (2015) whose experimental results indicated that the natural shells of mussels, sweet clams, and cockles had a calcium carbonate structure of orthorhombic, aragonite crystals. When heated above 500°C, the calcium carbonate structure changed its form to rhombohedral calcite crystals.

The results of the analysis of functional groups by measuring the absorption based on FTIR from the different shell powder samples in the 400-4000 cm^{-1} wavenumber range are shown in Figure 4. The detected peaks for NOSP, OSP_{700} and OSP_{800} had the same characteristics. The functional groups for the calcium carbonate in the oyster shell had wavenumbers at 713 and 875 cm^{-1} which indicated the peaks of the C–O function and the stretching oscillation mode of carbonate ion (CO_3^{2-}). The peak at

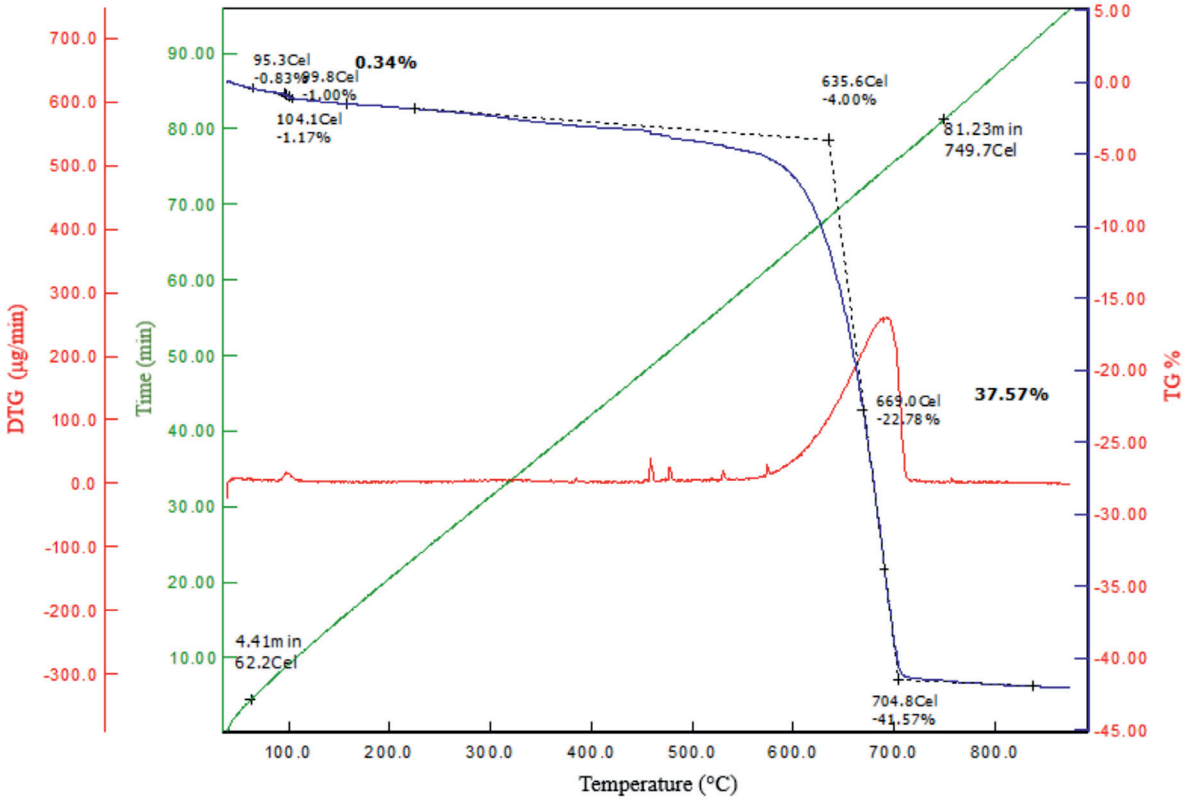

Fig 2. Thermogravimetric curves of natural oyster shell powder

713 cm^{-1} indicated the characteristics of calcite. On the other hand, the peak at 1419 cm^{-1} represented the C=O functional group, the stretching oscillation mode of CO_2 caused by the combustion process of CO_3^{2-} and CO_2 from the environment. In addition, there was a small peak at 1797 cm^{-1}, which indicated the C=O functional group, the stretching oscillation mode of CO_3^{2-}. The peak at 2515 cm^{-1} represented the C=O functional group with HCO_3^- stretching oscillation mode (Chang *et al.*, 2019). The peak at 2870 cm^{-1} belonged to the functional group of C–H, stretching oscillation mode of organic matter in the shell (Areeprasert *et al.*, 2014). When heated to 900°C, OSP_{900} decayed from calcium carbonate to calcium oxide and calcium hydroxide as indicated by the detection of the oscillation peak of the Ca=O functional group at approximately 523 cm^{-1} and the peak of the O–H functional group, the stretching oscillation mode of $Ca(OH)_2$ at approximately 3641 cm^{-1} (Choudhary *et al.*, 2015; Huh *et al.*, 2016). However, the peak of the C–H functional group was not found due to the complete decomposition of organic matter. These finding were consistent with the

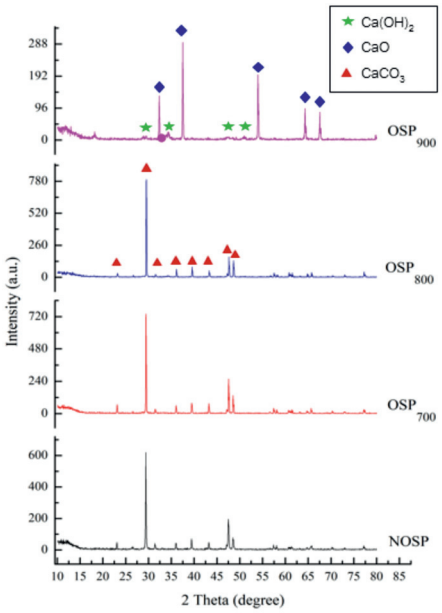

Fig 3. X-ray diffraction patterns of natural oyster shell powder (NOSP), oyster shell powder calcined at 700°C (OSP_{700}), oyster shell powder calcined at 800°C (OSP_{800}), and oyster shell powder calcined at 900°C (OSP_{900})

analysis of crystalline structural changes (using XRD) for calcium oxide, which is sensitive to hydrolysis, turning to $Ca(OH)_2$, as shown in the equation below, and having high alkalinity properties (Mohamed *et al.*, 2012; Oikawa *et al.*, 2000):

$$CaO\ (s) + H_2O\ (l) \rightleftharpoons Ca(OH)_2\ (s) + 15.2\ kcal$$

Antibacterial activity

The results of the study of antibacterial activity against *E. coli* and *S. aureus* by measuring the inhibition zone indicated no inhibition zones for NOSP and OSP_{700}. However, there were inhibition zones for OSP_{800} and OSP_{900} with both *E. coli* and *S. aureus* at all concentration levels. 5% of OSP_{900} achieved the highest antibacterial activity against both types of bacteria, as shown in Figure 5; this was consistent with the structure of OSP_{900} being calcium oxide and calcium hydroxide with high alkalinity, as well as the Ca=O functional group being ionized as a superoxide anion (O_2^-) and the O–H functional group being ionized as a hydroxyl ion (OH^-) with a strong reaction to the peptidoglycan of the bacterial membrane. This caused damage to the cell membranes of bacteria or DNA and the subsequent death of bacterial cells (Mohammadi *et al.*, 2012).

The quantitative antibacterial activity against *E. coli* and *S. aureus* at 5 and 30 minutes is shown in Table 3. OSP_{900} at 0% w/v concentration had no antibacterial activity against both types of bacteria. OSP_{900} at concentrations of 0.025, 0.05 and 0.1 % had antibacterial activity against *E. coli* and *S. aureus* that was significantly different from the activity of OSP_{900} at concentrations of 0.5, 0.75, and 1.0%. OSP_{900} at 0.5% w/v concentration entirely inhibited *E. coli* (Figure 6A, B and 7A, B). OSP_{900} at 1.0% w/v concentration entirely inhibited *S. aureus* (Figure 6C, D and 7C, D). The levels of antibacterial activity

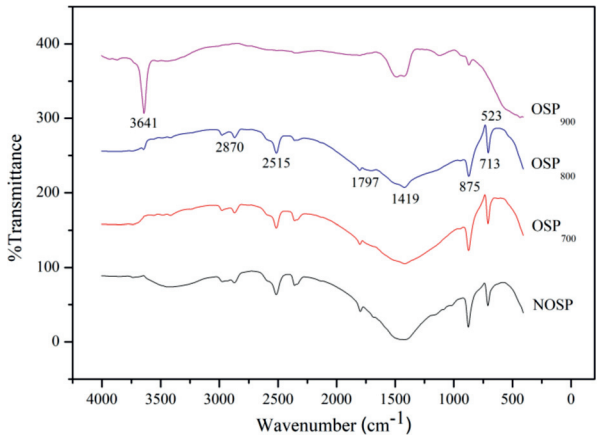

Fig. 4. Infrared spectra of natural oyster shell powder (NOSP), oyster shell powder calcined at 700°C (OSP_{700}), oyster shell powder calcined at 800°C (OSP_{800}) and oyster shell powder calcined at 900°C (OSP_{900})

(A) (B)

Fig. 5. Inhibition zone of natural oyster shell powder (NOSP), oyster shell powder calcined at 700°C (OSP_{700}), oyster shell powder calcined at 800°C (OSP_{800}) and oyster shell powder calcined at 900°C (OSP_{900}) on NA medium against: *E. coli* (A) and *S. aureus* (B) after 24-hour incubation at 37°C

Table 3. Antibacterial effects of OSP_{900} against *E. coli* and *S. aureus* at 5 and 30 minutes

OSP_{900} concentration (% w/v)	Bacterial count (CFU/mL)				Antibacterial activity (%)			
	E. coli 5 min	*S. aureus* 5 min	*E. coli* 30 min	*S. aureus* 30 min	*E. coli* 5 min	*S. aureus* 5 min	*E. coli* 30 min	*S. aureus* 30 min
0	3.2×10^5	9.0×10^6	1.6×10^5	2.7×10^5	0	0	0	0
0.025	3.0×10^5	7.0×10^6	3.9×10^4	2.6×10^5	57.90^a	19.60^a	77.50^a	12.67^a
0.05	2.5×10^5	6.0×10^6	3.5×10^4	2.6×10^5	63.13^a	28.60^{ab}	76.00^a	24.83^b
0.1	2.2×10^5	5.0×10^6	3.0×10^4	2.4×10^5	60.17^a	40.27^b	80.00^a	27.27^b
0.5	< 30	< 30	< 30	< 30	100.00^b	99.20^c	100.00^b	98.63^c
0.75	< 30	< 30	< 30	< 30	100.00^b	99.97^c	100.00^b	98.20^c
1.0	< 30	< 30	< 30	< 30	100.00^b	100.00^c	100.00^b	100.00^c

Note: Different letters within a column indicate significant differences ($p < 0.05$)

against *E. coli* and *S. aureus* at 5 minutes of exposure time were not significantly different. In contrast, at 30 minutes exposure time, the antibacterial activity against *E. coli* was significantly higher than that against *S. aureus*. This finding was consistent with the structural characteristics of Gram-positive bacteria having 90% of the cell membrane composed of peptidoglycans and its teichoic acid linking to peptidoglycans which increases the strength of the cell membrane that are thicker than for Gram-negative bacteria as well as the cells membrane containing unsaturated fatty acid called Lipopolysaccharide which enables for an easily oxidation process by hydroxyl ion (OH^-) and superoxide ion (O_2^-) that are formed by Ca=O functional group in the lipid peroxidation. Consequently, inhibition of *E. coli* was easier than that of *S. aureus* (Peng *et al.*, 2010).

Antibacterial activity against bacteria in vegetables

The antibacterial activity of OSP_{900} against *E. coli* in bean sprouts and lettuce for 5 minutes is shown in Figure 8 and Table 4. At the 0% w/v concentration of OSP_{900} level, the growth of *E. coli* colonies on solid EMB agar was observed as many small black dots in the middle and a metallic sheen. Testing for antibac-

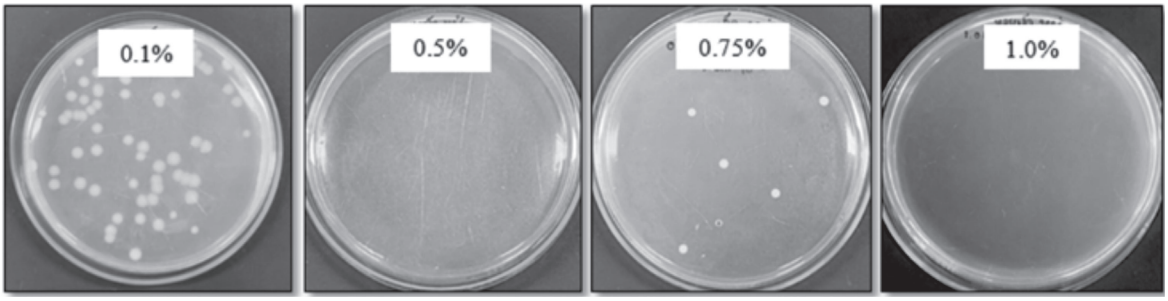

Fig. 6. Colonies of bacteria on PCA medium with OSP_{900} at 5 minutes of exposure time: 0.1% w/v OSP_{900} / *E. coli* (A), 0.5% w/v OSP_{900} /*E. coli* (B), 0.75% w/v OSP900 /*S. aureus* (C) and 1.0% w/v OSP900 /*S. aureus* (D)

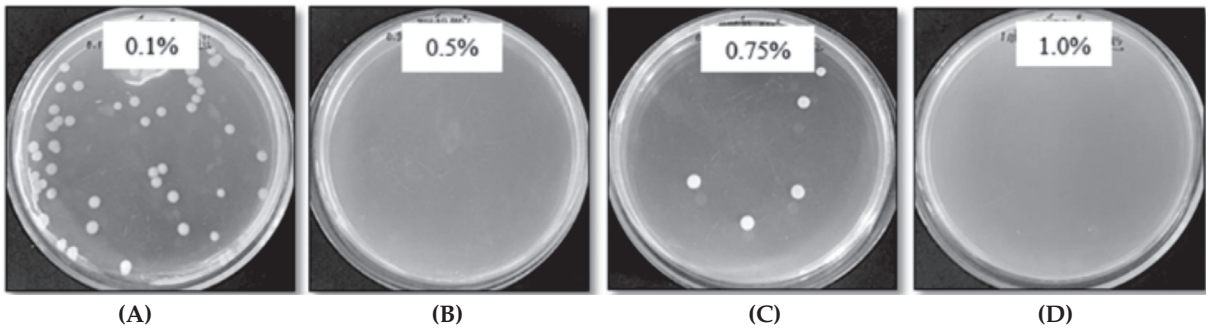

Fig. 7. Colonies of bacteria on PCA medium with OSP_{900} for 30 minutes of exposure time: 0.1% w/v OSP_{900} /*E. coli* (A), 0.5% w/v OSP_{900} / *E. coli* (B) 0.75% w/v OSP_{900} /*S. aureus* (C) and 1.0% w/v OSP_{900} /*S. aureus* (D)

Table 4. *Escherichia coli* counts for bean sprouts and lettuce soaked in solutions of antibacterial agent (OSP_{900}) for 5 minutes

OSP_{900} concentration (% w/v)	Dilution	Bean sprouts		Lettuce	
		E. coli (CFU/g)	Antibacterial activity (%)	*E. coli* (CFU/g)	Antibacterial activity (%)
0	1×10^2	> 300	-	> 300	-
0.25	1×10^2	< 30	98.6	< 30	99.2
0.50	1×10^2	< 30	100	< 30	100
1.0	1×10^2	< 30	100	< 30	100

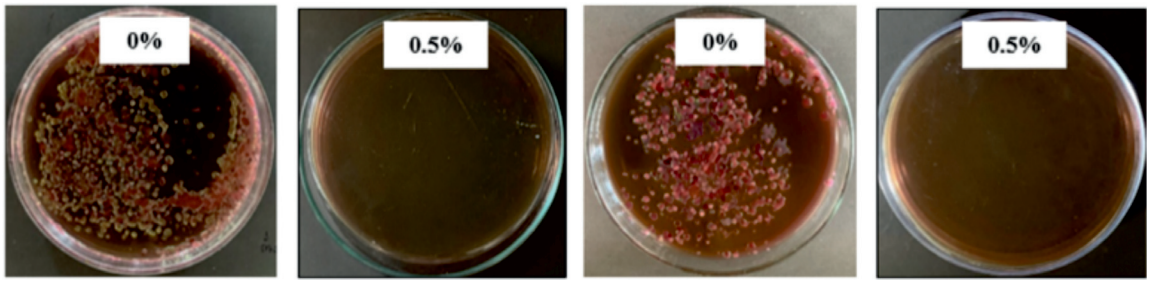

(A) (B) (C) (D)

Fig. 8. Colonies of bacteria on EMB agr with OSP_{900} used to soak bean sprouts and lettuce: 0% w/v OSP_{900} / been sprout (A), 0.5% w/v OSP_{900} /bean sprout (B), 0% w/v OSP_{900} / lettuce (C) and 0.5% w/v OSP_{900} lettuce (D)

terial activity against *E. coli* at concentrations of OSP_{900} at 0.25, 0.5 and 1.0% indicated that *E. coli* was inhibited in both bean sprouts and lettuce at all concentration levels. The 100% inhibition level was reached at the concentration of OSP_{900} at 0.5 % w/v, in line with Oikawa *et al*. (2000) where calcium oxide produced by wild surf clams had antibacterial activity against coliform bacteria in vegetables. Therefore, based on this study, OSP_{900} produced from natural materials and used in a small amount to soak vegetables before consumption for only 5 minutes could effectively inhibit bacterial contamination in fresh vegetables.

Conclusion

This study on calcium oxide from *Saccostrea cucullata* shells demonstrated the important role of the calcination temperature in the structural changes in calcium carbonate. Natural oyster shell powder (NOSP) and shell powder calcined at a low temperatures of 700°C (OSP_{700}) and 800°C (OSP_{800}) had an original structure of calcium carbonate. However, when heated to 900°C (OSP_{900}), the structure changed from calcium carbonate to calcium oxide and calcium hydroxide and had antibacterial activity against *E. coli and S. aureus*. Qualitatively, the inhibition on *E. coli* zone was visible in testing. Quantitatively, 0.5% w/v concentration of OSP_{900} produced 100% inhibition on *E. coli*, at 5 minutes of exposure time. For *S. aureus*, the same inhibitory effect was evident at OSP_{900} for a concentration of 1.0% w/v at 30 minutes of exposure time. *E. coli* in bean sprouts and lettuce was 100% inhibited at a concentration of 0.5% w/v based on a 5 minute infusion of the fresh vegetables.

Acknowledgement

Material and equipment used in this research were provided by Department of Science and Environmental Technology, Faculty of Science at Sriracha, Kasetsart University, Chonburi, Thailand. Additional support was provided by the Scientific Instruments Center, Faculty of Science, King Mongkut's Institute of Technology, Ladkrabang, Thailand.

References

Alidoust, D., Kawahigashi, M., Yoshizawa, S., Sumida, H. and Watanabe, M. 2015. Mechanism of cadmium biosorption from aqueous solutions using calcined oyster shells. *Environmental Management*. 150 : 103-110.

American Public Health Association, 2015. *Compendium of Methods for Microbiological Examination of Foods*. 5th ed. Apha Press, Washington, DC.

American Society for Testing and Materials. 2001. ASTM E2149-01: Standard test method for determining the antimicrobial activity of immobilized antimicrobial agent under dynamic contact conditions. ASTM International, West Conshohocken, PA.

Areeprasert, C., Zhao, P., Ma, D., Shen, Y. and Yoshikawa, K. 2014. Alternative solid fuel production from paper sludge employing hydrothermal treatment. *Energy and Fuel*. 28 : 1198-1206.

Boonyuen, S., Malaithong, M., Phokaew, A., Cherdhirunkorn, B. and Chuasantia, I. 2015. Decomposition of calcium carbonate in shells. *Thai Journal of Science and Technology*. 4(2): 115-122.

Chammanee, P., Sombatsopop, K., Kositchaiyong, A. and Sombatsompop, N. 2009. Effects of anti-bacterial agents, sample preparation and contact time on antibacterial efficacy in MDPE film. *Journal of Macromolecular Science*. 48 : 755–765.

Chang, H.Y.H., Kuo, Y.L. and. Liu, J.C. 2019. Fluoride at

waste oyster shell surfaces – Role of magnesium. *The Total Environment*. 652 : 1331-1338.

Choudhary, R., Koppala, S. and Swamiappan, S. 2015. Bioactivity studies of calcium magnesium silicate prepared from eggshell waste by sol–gel combustion synthesis. *Journal of Asian Ceramic Societies.* 145 : 173-177.

Dangkanid, T. 1995. *Posthavest changes and quality of durians cv. montong repened at different temperatures*. M.S. Thesis, Graduate School, Kasetsart University, Bangkok, Thailand.

Fisheries Statistics of Thailand. 2017. *Fisheries development policy and strategy division*. Department of Fisheries. Ministry of Agriculture and Cooperatives, Bangkok, Thailand. 92 p.

Huh, J.H., Choi, Y.H., Ramakrishna, C., Cheong, S.H. and Ahn, J.W. 2016. Use of calcined oyster shell powders as CO_2 adsorbents in algae-containing water. *The Korean Ceramic Society*. 53(4) : 429-434.

Kositchaiyong, A., Thongpin, C., Sombatsompop, K., Chandavasu, C., Markpin, T., Wimolmala, E. and Sombatsompop, N. 2010. Material characterizations and anti-bacterial performances of triclosan containing high-density polyethylene. *Research and Innovation for Thai Industries*. 1 : 16-27.

Miller, C.H., Stuart, K.G., Brown Jr, C.E. and Newton, C.W. 2012. The comparative antimicrobial effect of calcium hydroxide. *Oral Surgery, Oral Medicine, Oral Pathology.* 72: 101-104.

Mohamed, M., Yusup, S. and Maitra, S. 2012. Decomposition study of calcium carbonate in Cockle shell. *Engineering Science and Technology.* 7(1) : 1-10.

Mohammadi, Z., Shalavi, S. and Yazdizadeh, M. 2012. Antimicrobial activity of calcium hydroxide in endodontics: A review. *Chonnam Medical.* 48 : 133-140.

Nataro, J.P., Strockbine, N.A., Bopp, C.A., Fields, P.I. and Kaper, J.B. 2011. *Escherichia, Shigella and Salmonella. Clinical Microbiology*. 37 : 685-713.

Oikawa, K., Asada, T., Yamamoto, K., Wakabayashi, H., Sasaki, M., Sato, M. and Matsuda, J. 2000. Antibacterial activity of calcined shell calcium prepared from wild surf clam. *Health Science.* 46(2) : 98-103.

Peng L., W. Duan, Q., Wang and X. Li. 2010. The damage of outer membrane of *Escherichia coil* in the presence of TiO_2 combine with UV light. C*olloids and surface B: Biointerface*. 78 : 171-176.

Roy, A., Gauri, S.S., Bhattacharya, M. and Bhattacharya, J. 2013. Antimicrobial activity of CaO nanoparticles. *Journal of Biomedical Nanotechnology.* 9 : 1-8.

Tapaneeyakul, N. and Kongsuk, W. 2015. *Staphylococcus aureus*. Research and laboratory development center. Ministry of public health, Bangkok, Thailand.

Tsou, C.H., Wu, C.S., Hung, W.S., Guzman, M.R.D., Gao, C., Wang, R.Y., Chen, J., Wan, N. Peng, Y.J. and Suen, M.C. 2018. Rendering polypropylene biocomposites antibacterial through modification with oyster shell powder. *Polymer.* 160 : 265-271.

Yen, H.Y. and Li., J.Y. 2015. Process optimization for Ni(II) removal from wastewater by calcined oyster shell powders using Taguchi method. *Journal of Environmental Management*. 161 : 344-349.

Yoon, G.L., Kim, B.T., Kim, B.O. and Han, S.H. 2003. Chemical–mechanical characteristics of crushed oyster-shell. *Waste Management*. 23 : 825–834.